



# LUND UNIVERSITY

## Analysis of Porosity and Tortuosity in a 2D Selected Region of Solid Oxide Fuel Cell Cathode Using the Lattice Boltzmann Method

Espinoza Andaluz, Mayken; Sundén, Bengt; Andersson, Martin; Yuan, Jinliang

*Published in:*  
ECS Transactions

*DOI:*  
[10.1149/06501.0059ecst](https://doi.org/10.1149/06501.0059ecst)

2015

[Link to publication](#)

*Citation for published version (APA):*

Espinoza Andaluz, M., Sundén, B., Andersson, M., & Yuan, J. (2015). Analysis of Porosity and Tortuosity in a 2D Selected Region of Solid Oxide Fuel Cell Cathode Using the Lattice Boltzmann Method. In *ECS Transactions* (Vol. 65, pp. 59-73). Electrochemical Society. <https://doi.org/10.1149/06501.0059ecst>

*Total number of authors:*  
4

### General rights

Unless other specific re-use rights are stated the following general rights apply:  
Copyright and moral rights for the publications made accessible in the public portal are retained by the authors and/or other copyright owners and it is a condition of accessing publications that users recognise and abide by the legal requirements associated with these rights.

- Users may download and print one copy of any publication from the public portal for the purpose of private study or research.
- You may not further distribute the material or use it for any profit-making activity or commercial gain
- You may freely distribute the URL identifying the publication in the public portal

Read more about Creative commons licenses: <https://creativecommons.org/licenses/>

### Take down policy

If you believe that this document breaches copyright please contact us providing details, and we will remove access to the work immediately and investigate your claim.

LUND UNIVERSITY

PO Box 117  
221 00 Lund  
+46 46-222 00 00

## Analysis of Porosity and Tortuosity in a 2D Selected Region of Solid Oxide Fuel Cell Cathode Using the Lattice Boltzmann Method

M. Espinoza<sup>a</sup>, B. Sundén<sup>b</sup>, M. Andersson<sup>c</sup>, and J. Yuan<sup>d</sup>

<sup>a,b,c,d</sup> Department of Energy Sciences, Lund University, Lund, SE-221 00, Sweden

The solid oxide fuel cell (SOFC) is one of the most promising devices for getting electrical energy. There are a lot of advantages in the use of SOFCs such as their efficiency, higher electrical and thermal power production and reduction of the emission of polluting gases.

Modeling the SOFC at downscale is one of the most important challenges in fuel cell (FC) research. Knowing the behavior of materials to this scale is a helpful tool to predict the physical and chemical phenomena within the FCs, improve their efficiency and reduce material costs.

At micro- and mesoscale, Lattice Boltzmann Method (LBM) appears as a powerful tool for modeling fuel cells. LBM has been proven suitable for solving several physical phenomena in complex geometries such as porous media.

Using the D2Q9 LBM scheme, the velocity field for a selected section of an SOFC cathode is determined. This velocity field is shown in 2D and 3D graphics. The porosity and tortuosity for this selected region are calculated and compared with previous results.

### Introduction

The behavior of the fluid flow in complex geometries is considered an issue for modeling different transport phenomena. In the SOFC, the analysis of the porous domain present in the electrodes plays an important role in the energy conversion process.

The first part of this paper describes the principles, basic characteristics and advantages of the Lattice Boltzmann Method. The most common schemes for solving the Boltzmann equation and the scheme applied in the current work are shown. Two principal parameters studied in porous media, i.e., porosity and tortuosity, are defined. In the second part general information related to the Boltzmann equation and some previous studies related to this current work are given.

Then, the selection of the domain where the velocity field was solved and the process for image reconstruction are presented. The last part of this paper shows the porosity and tortuosity values obtained in this work and the comparison of these values with previous porosity-tortuosity relationship.

### LBM Basics

During recent years, Lattice Boltzmann Method (LBM) applications have been having more presence in several fields of research. The scheme is successful in fluid flow applications and complex boundaries (1).

LBM is based originally from lattice gas automata (LGA). This method analyzes its own physical states and the states of some of its neighbors (2). The number of neighbors used in the model is defined depending on the problem to be solved. The main idea of LBM is to study the behavior of a collection of particles instead of a single sub-atomic particle like in molecular dynamics (MD). LBM can be considered as a bridge between the continuum methods and discrete methods.

Knowing the average characteristics of the collection of particles; it is possible to make approximations with considerable accuracy of the different physical phenomena, not only at the microscale, but also at the macroscale level (3).

The analysis of the movement of millions of atomic particles is simplified using the particle distribution function (PDF). The PDF gives a statistical description of the collection of particles and in consequence the principal characteristics of the fluid behavior. The PDF is a function of the position and time of the group of particles.

The domain that will be solved has to be divided into lattice points, as well called lattice nodes. Each lattice point has velocity connections with its neighborhood. The common way to represent the lattice arrangement is  $DmQn$  where  $m$  is related to the dimension of the problem to be solved (1-D, 2-D or 3-D) and  $n$  determines the number of connections with the other lattice nodes.

Each velocity connection has a corresponding weighting factor that depends on the total number of connections between the nodes. The total sum of the weighting factors must always be the unity. The schemes of LBM often used are D2Q9 and D3Q19; they are represented in Figure 1. In this work the scheme D2Q9 is applied for solving the velocity field.

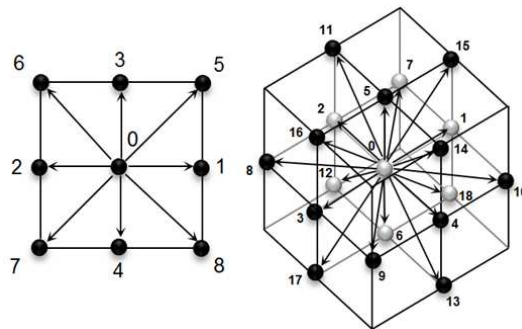


Figure 1. Most common lattice arrangements applied in LBM. D2Q9 (left) and D3Q19 (right).

LBM presents many advantages in the modeling of different processes in several research fields. LBM can be used to solve problems related to single- and multi-phase flows, unsteady flows, and heat transport (2). Comparing Navier-Stokes equation and Boltzmann equation, the first one is a second - order differential equation where it is necessary to treat the non-linear convective term; the Boltzmann equation, however, is a first - order differential equation and avoids the convective term (3).

This method is useful in predicting and visualizing physical processes and microstructures (4). LBM is a suitable candidate for efficient parallel computations due to the algorithm used in solving the problems (5). LBM is a useful tool for mesoscale modeling of single- and multi-phase flow (6), e.g., two-phase flow in mixing layers, electro-osmotic flow, and viscous fingering phenomena. LBM is computationally more efficient than the finite difference method for the same grid size (7).

The results of investigations show that LBM is a viable alternative solution method to traditional numerical methods for solving flow problems in heterogeneous porous media (8). Some parameters involved in the porous media will be described in the next section.

### Variables Studied

Porosity. The porosity ( $\phi$ ) in the porous media is defined as the fraction of the total volume that is occupied by void space (9). To calculate porosity, it can be expressed by one simple equation:

$$\phi = \frac{\text{void Volume}}{\text{total Volume}} \quad [1]$$

Based on the above equation is easy to conclude that the porosity values are always lower than one. The porosity is a dimensionless parameter.

In this work the velocity field for a two dimensional case is solved, therefore the porosity is defined as the ratio between the void surface (part of the domain without solid material) and the total surface.

The behavior of the fluid flow through the pore domain depends on porosity value. The next pictures show the velocity field in materials with two different porosities (this way, the reader has a general idea of this quantity and its incidence). In both examples, the solid material is represented by groups of small squares (1 lattice unit) and they are placed in selected positions inside the domain.

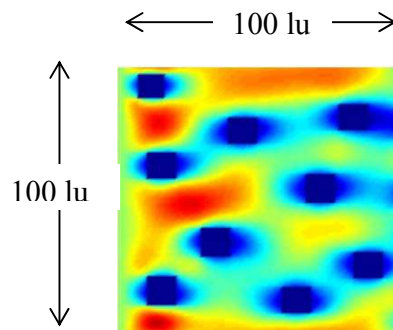


Figure 2. Behavior of the fluid in an aleatory porous domain with porosity  $\phi_1=0.90$ . (Red color higher velocities, blue color lower velocities)

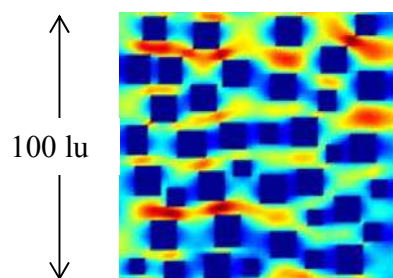


Figure 3. Behavior of the fluid in an aleatory porous domain with porosity  $\phi_2=0.67$ . (Red color higher velocities, blue color lower velocities)

The porous material in Figure 2 has porosity  $\phi_1$  and the material in the Figure 3 has porosity  $\phi_2$ . According to the model,  $\phi_1$  is greater than  $\phi_2$ , that is, the void space has more presence in the material of Figure 2.

Tortuosity. Tortuosity is one of the key parameters to study in the porous media. Tortuosity is defined as the ratio of the length of the actual path of the fluid particles to the shortest path length in the direction of the flow (10).

$$\tau = \frac{L_{actual}}{L_{shortest}} \quad [2]$$

Tortuosity value is always greater than one. However, must be the unity when the actual length path is equal to the shortest path length (domain with no obstacles). The tortuosity, similar to the porosity, is a dimensionless parameter.

According to Sousa and Nabovati (11), the tortuosity can be calculated using the next equation:

$$\tau = \frac{\sum_{i,j} u_{mag}(i,j)}{\sum_{i,j} |u_x(i,j)|} \quad [3]$$

where the flow is in x-direction.

In Eq. [3] it is necessary to calculate the velocity magnitude for each node, which is calculated by definition:

$$u_{mag}(i,j) = \sqrt{u_x(i,j)^2 + u_y(i,j)^2} \quad [4]$$

One of the issues treated in previous studies has been to find a relationship between the porosity and tortuosity. The next section presents some of these relationships.

Relation between tortuosity and porosity. There are several relationships between tortuosity and porosity. Some of these relations are based on experimental data and others are on theoretical equations.

Koponen et al. (12), have proposed a linear relation between the tortuosity and porosity. The next equation shows the relationship.

$$\tau = 0.8(1 - \phi) + 1 \quad [5]$$

where  $\phi$  is the porosity of the material.

Based on simulation results Koponen et al. (13) found an a more complex expression with the inclusion of some fitting values. The corrected relation is expressed as:

$$\tau = 1 + a \frac{(1 - \phi)}{(\phi - \phi_c)^m} \quad [6]$$

where  $\phi_c$ ,  $m$  and  $a$  are 0.33, 0.65 and 0.19 respectively.

Sousa and Nabovati (11), proposed a different relationship between the tortuosity and porosity. In this relation the variables are related in function of one polynomial equation. The equation is established as follows:

$$\tau = -0.5191\phi^3 + 0.879\phi^2 - 1.1657\phi + 1.8058 \quad [7]$$

According to the results of Barrande et al. (14), the relation between the variables in mention; is obtained using a logarithmical function. The tortuosity can be expressed as:

$$\tau = 1 - 0.49 \ln(\phi) \quad [8]$$

It is important to notice that in the literature the tortuosity is defined in different ways. Some relationships are based on experimental measurements and another are theoretical ones. The definition of tortuosity in general way comes from the Eq. [2] and expressed in function of the velocities is in the Eq. [3].

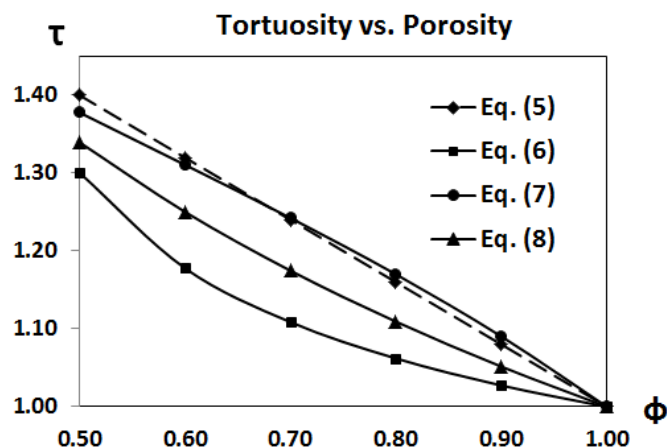


Figure 4. Four different relationships between the tortuosity and the porosity.

Figure 4 presents the four previous relationships mentioned. The range values of porosity shown is between 0.5 and 1. The picture shows that tortuosity increases while

porosity decreases, and in the theoretical case when the porosity is one, i.e., there is no any solid material neither obstacles, the tortuosity must be one.

Porous media in FCs. There are some parts of FCs that are made up of porous materials. The study of the characteristics of these structures is of vital importance to have a deep understanding of the physical and chemical phenomena that occur within FCs during the energy conversion process. Moreover, the knowledge acquired at microscale will help to the coupling of the different scales in FC modeling.

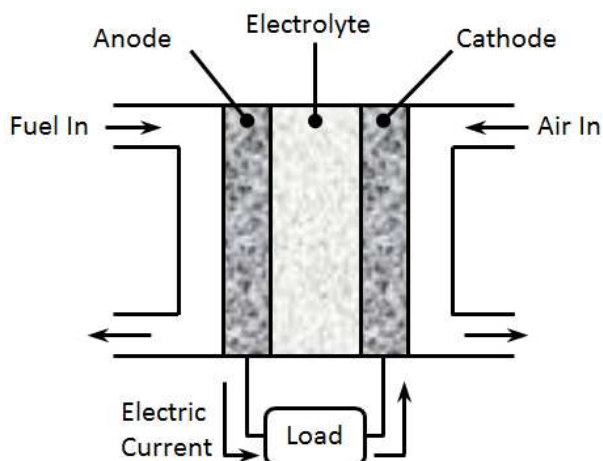


Figure 5. General scheme of a single Fuel Cell

Figure 5 shows a general FC structure and their components. The next table presents the different parts of FCs with their respective range of porosity values found in the literature.

**TABLE I.** Fuel cell components and their porosity

| PEMFC                                     |  | $\phi$      |
|---|--|-------------|
| Gas diffusion layer (GDL) <sup>(15)</sup> |  | 0.60 ~ 0.90 |
| Catalyst layer (CL) <sup>(16)</sup>       |  | 0.40 ~ 0.60 |
| SOFC                                      |  | $\phi$      |
| Support layer <sup>(17)</sup>             |  | 0.36 ~ 0.38 |
| Anode/Cathode <sup>(16)</sup>             |  | 0.30 ~ 0.40 |

The porosity in FC parts falls in the range 0.30 – 0.90. This characteristic allows the gases involved in the energy conversion process, i.e., Oxygen, Hydrogen, Methane, Carbon Dioxide, etc. getting in contact with the electrolyte (proton exchange membrane in PEMFC and solid electrolyte in SOFC).

Due to the nature of the manufacturing, the parts of the FCs showed in Table I are commonly anisotropic and with inhomogeneous structure (18). The porosity has incidence over the heat and mass transport phenomena that occur within the FCs.



## Methodology

According to the Table 1, the porous media are present in different parts of the FCs, (i.e., GDLs, CLs, and electrodes). The study and modeling of the behavior of fluids throughout a porous media are of vital importance in the understanding of the FCs. Figure 6 shows the porous structure of an SOFC cathode.

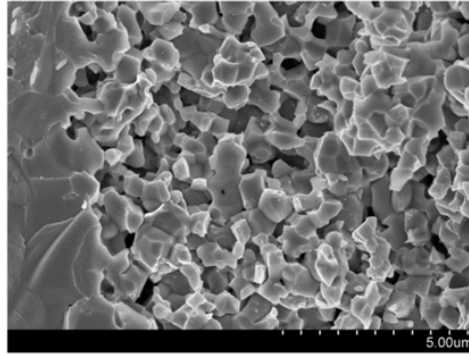


Figure 6. SEM micrograph shows the porous structure of a SOFC cathode. Credits: Ningbo Institute of Materials Technology & Engineering (NIMTE).

One objective of this project is to study the behavior of the fluid flow in the porous media, specifically the velocity field is calculated. Another objective includes: to calculate the porosity and tortuosity for a specific section of the pore domain, and compare with previous results. These results show to LBM as a powerful tool for handling flows in micro-structures.

The backbone of LBM is the Boltzmann transport equation, which is based on the distribution function. The particle distribution function (PDF) corresponds to the number of particles in a determined region within a range of velocities at one specific time. The PDF remains the same if there is no collision between the molecules (streaming); otherwise, it will have a net change in the distribution function (collision).

A simplified form of the Boltzmann equation can be expressed as:

$$\frac{\partial f(r, t)}{\partial t} + c \cdot \nabla f(r, t) = \Omega \quad [9]$$

where  $f$  is the particle distribution function that depends on position, velocity  $c$  and time  $t$ .  $\Omega$  is the collision operator that is a function of  $f$ .

To solve the Boltzmann equation, one approximation is used for replacing  $\Omega$ ; this approximation is called the Bhatnagar, Gross, and Krook (BGK) approximation. Then, Eq. [9] can be expressed as:

$$\frac{\partial f_i(r, t)}{\partial t} + c_i \nabla f_i(r, t) = \frac{1}{\tau_1} [f_i^{eq}(r, t) - f_i(r, t)] \quad [10]$$



where  $f_i(r,t)$  is the particle distribution function at position  $r$  and time  $t$ ;  $f_i^{eq}(r,t)$  is the equilibrium particle distribution function and  $\tau_i$  is the relaxation time,  $c_i$  is the velocity in the corresponding  $i$ - direction.

To solve Eq. [10], it is necessary to define the equilibrium particle distribution function ( $f_i^{eq}$ ) in a different way for each problem to be solved. LBM can solve the diffusion, advection-diffusion, momentum, and energy equations. The equilibrium particle distribution function comes from a Taylor polynomial approximation and Maxwell's distribution function, and can be written as (3):

$$f_i^{eq} = \phi w_i [A + B c_i \cdot u + C (c_i \cdot u)^2 + D u^2] \quad [11]$$

where  $u$  is the macroscopic velocity vector,  $w_i$  is the weighting factor, and A, B, C and D have to be defined based on the conservation equation that is applied.  $\Phi$  is a scalar parameter that often refers to density, temperature or species concentration.

In this work the momentum equation was solved. Under these conditions Eq. [11] has to be written as (3):

$$f_i^{eq} = rho(i,j)w_i [1 + 3 * t2_i(i,j) + 4.5 * t2_i(i,j) * t2_i(i,j) - 1.5 * t1(i,j)] \quad [12]$$

where  $t1(i,j)$  is the dot product of the local velocity in the position  $(i,j)$  with itself and  $t2_i(i,j)$  acquires values depending on the dot product of the velocities in the  $i$ - direction.

Once Eq. [10] is solved, it is possible to recover macroscopic parameters such as density, velocity and momentum. Equation 13 shows how to recover the macroscopic velocity field.

$$u = \frac{1}{\rho} \sum_{i=0}^{n-1} f_i c_i \quad [13]$$

Using the velocity field, based on the Eq. [3] the tortuosity is calculated. The calculation of the selected region is computed using the Eq. [1] but for the 2D case.

The study of porous media is important in modeling and experimental research. There is an extensive quantity of previous studies concerning the fabrication, reconstruction and modeling of different parts of the FCs. As shown in Table I, several parts of the FCs are of a porous nature.

The following table shows some of investigations related to porous media applied into the FCs. The researches shown are focused on different parts of the PEMFCs and SOFC involved in the energy conversion process such as: electrodes, GDL, CL and support layers.

**TABLE II.** Summary of researches of porous media in FCs

| FC type        | Principal aspects researched   | FC part analyzed |
|----------------|--|------------------|
| PEMFC          | Effects of porosity distribution variation on fuel cell performance (19)   | GDL              |
| FCs in general | Characterization of Porosity of Electrodes and Separators in Fuel Cell Industry (20)   | electrodes       |
| PEMFC          | Description of the coupling of the free flow in the channel region with filtration velocity in the porous diffusion layer (21)               | GDL              |
| PEMFC          | The effects of the various porous electrode design parameters such as: porosity, solid electronic conductivity and thermal conductivity (22) | GDL, CL          |
| SOFC           | A porous yttria-stabilized zirconia (YSZ) ceramic supported single cell was fabricated in order to measure power and current densities (17)  | Support layer    |
| SOFC           | A phase field method was used to simulate the microstructural evolution of nickel-yttria stabilized zirconia composite anode (23)            | Anode            |
| SOFC           | A Numerical solution method was developed to reconstruct and evaluate the porous anode (24)  | Anode            |
| SOFC           | An anode supported was fabricated and characterized as a function of the components in the anode supports (25)                               | Anode            |
| SOFC           | The effect of thickness, porosity, pore size, and pore tortuosity on fuel and exhaust gas flow was calculated. (26)                          | Anode            |
| PEMFC          | The effect of porosity heterogeneity on the bulk hydrodynamic properties (permeability and tortuosity) (27)                                  | GDL              |

### Image Reconstruction

The first step to getting the velocity field in the porous media is to convert the grayscale image into a black-white scale with 50% of saturation; a black color represents the void spaces and a white color represents the solid material.

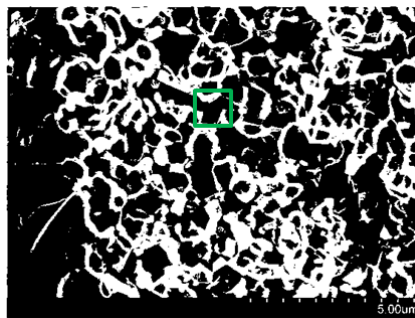


Figure 7. Picture of the SOFC cathode after the conversion to black-white scale and region selected to model.

The selected region corresponds to a square surface area of  $10\ \mu\text{m} \times 10\ \mu\text{m}$ . To show the specific region where the fluid flow is modeled, Figure 8 presents only the green square of  $100\ \mu\text{m}^2$ .

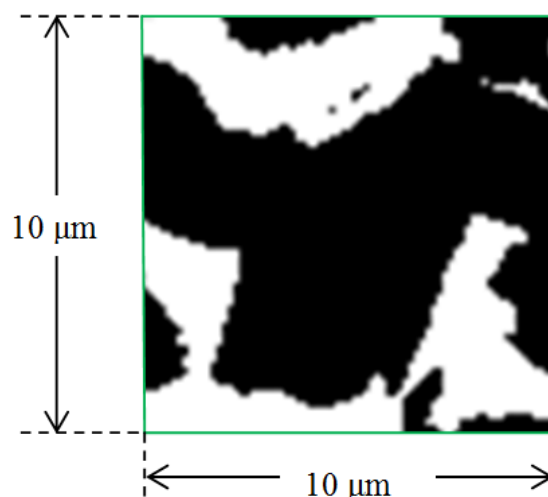


Figure 8. The region where the velocity field is solved using LBM. (Black: void spaces, white: solid material)

Using graphical software functions, the image is acquired and translated into a binary image. The solid material is represented by ones and void spaces are represented by zeros. In the nodes where the solid materials is present, bounce-back boundary conditions were implemented.

## Results and Discussions

Once the momentum equation was solved using the LBM to calculate the velocity field, Figure 9 shows the velocity vectors in blue color. The fluid flow was established in the direction from left to right.

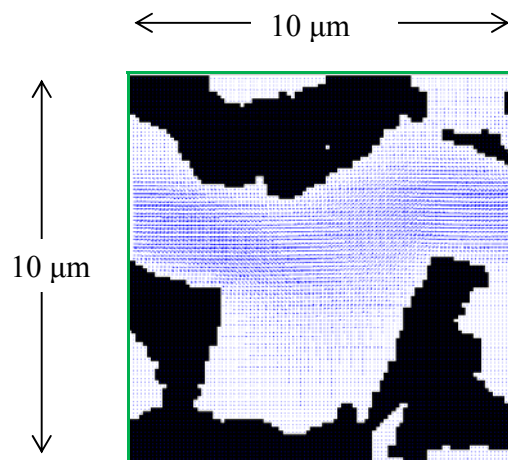


Figure 9. Velocity field vector [lu/ts] for the selected region of the SOFC cathode (black: solid material, white: void spaces)

According to the definition of porosity showed in the previous section and taking into account the void spaces and solid materials presented in the selected region, the porosity of this section is calculated using Eq. [6]. Then the porosity value is  $\phi=0.59$ .

The model gives, as a result, the velocity values for each lattice node expressed in their components (i.e., x-direction and y-direction). Treating these values and using Eq. [4], the velocity magnitude is calculated.

For each lattice node, its velocity magnitude is calculated and expressed using a color scale. These results are shown in a two-dimensional image in Figure 10 whereas in Figure 11 a three-dimensional representation of the velocity field is presented. The velocities are presented with a normalized value taking as reference the maximum velocity value.

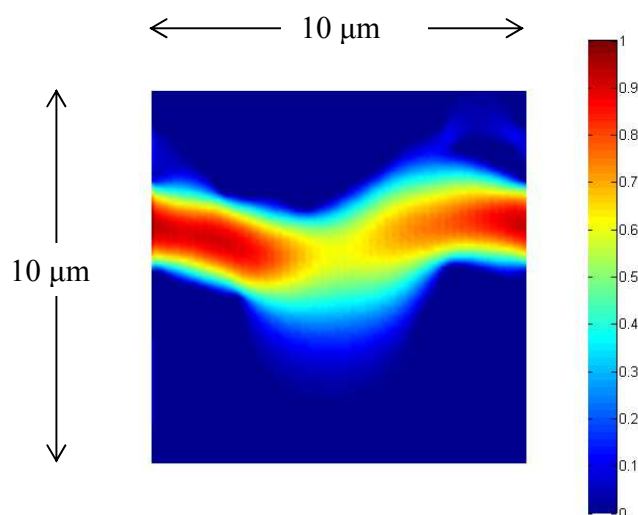


Figure 10. Two-dimensional representation of the normalized velocity for each lattice position.

The pictures show that in the presence of solid material, the velocity magnitude is equal to zero, and this was expected. The highest values of velocities are found in the narrow region.

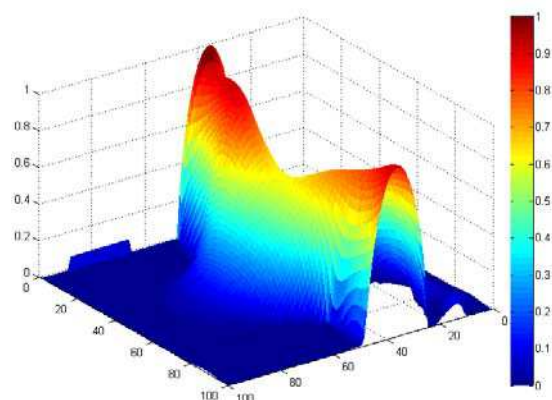


Figure 11. Three-dimensional representation of the relative velocity magnitude for each lattice position.

According to the definition of tortuosity (Eq. [3]), using the known velocities and the velocity magnitude in each position ( $i,j$ ), the value calculated is  $\tau=1.18$ .

To compare the values obtained in this study with the relationships previously found by different authors, Figure 12 shows the result together with the relationship curves; i.e., tortuosity versus porosity.

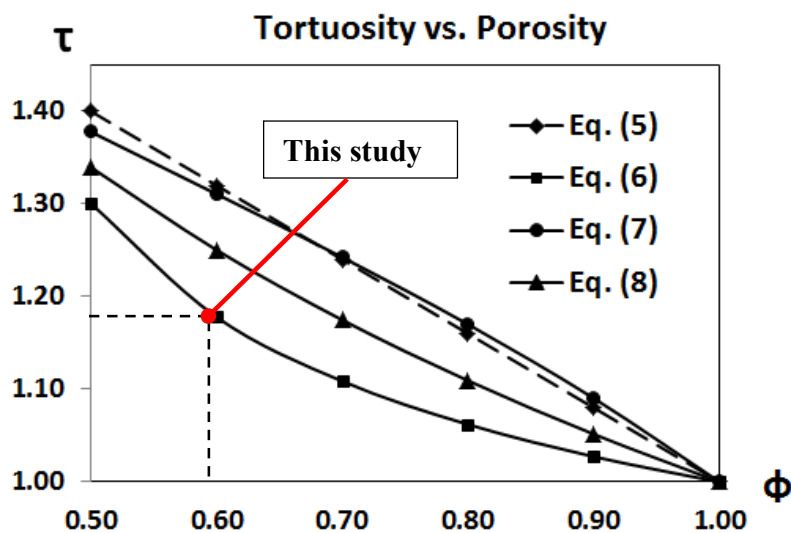


Figure 12. Values of tortuosity (1.18) and porosity (0.59) calculated for the selected region of SOFC cathode, and the relationships previously found.

Using the equations in previous studies, (i.e., Equations [5], [6], [7], and [8]) and replacing the porosity calculated of the material, the tortuosity for each relation is obtained. The different values of tortuosity are presented in the next table.

**TABLE III.** Comparison between the result obtained in this study and the previous studies related to porosity and tortuosity.

| Porosity<br>- $\phi$ - | Tortuosity<br>- $\tau$ - | Percent deviation |
|------------------------|--------------------------|-------------------|
| 0.59                   | Eq. [5]                  | 1.33              |
|                        | Eq. [6]                  | 1.19              |
|                        | Eq. [7]                  | 1.32              |
|                        | Eq. [8]                  | 1.26              |
|                        | This study               | 1.18              |

Considering the results in Table III, the percent variation with respect to the previous results are lower than 11.0 %. The closest value is obtained with Eq. [6] proposed by Koponen et al. (13), with a percent deviation lower than 1.0 %.

Sousa and Nabovati (11) showed some values of predicted tortuosity as a function of the porosity (Fig. 13). The result of the present study falls in the region of the predicted tortuosity values.

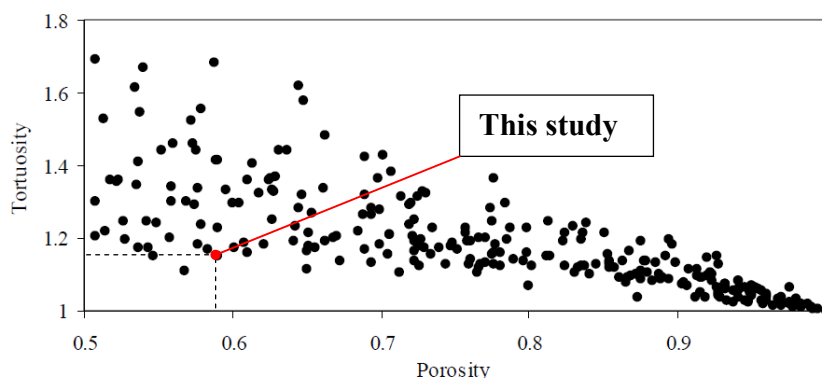


Figure 13. Predicted tortuosity as a function of the porosity (black dots) from Nabovati *et al.* (11), and result of this study (red dot).

## Conclusions

A 2D velocity field for one selected SOFC cathode region was solved. The LBM scheme used for solving the velocity field is D2Q9. The selected region was of  $100 \mu\text{m}^2$ . The model was implemented in Matlab. LBM has demonstrated to be a powerful tool for modelling fluid flows in porous media.

The porosity is a physical characteristic presents in different parts of the FCs. Studying and analyzing the incidence of the tortuosity in the mass and heat transfer phenomena is helpful for getting a complete description of the FC systems.

The porosity was calculated using the reconstructed 2D image of the SEM cathode picture. The velocity field was the point of departure in the calculation of the tortuosity.

The porosity and tortuosity found in the selected region were 0.59 and 1.18 respectively. The tortuosity calculated is an acceptable value in comparison with the previous findings, i.e., within 0.4 % and 11 % deviation compared with previous results.

The common porosity values in the FCs parts are included between 0.3 and 0.9. It was found that the tortuosity is related to the porosity but not directly. The tortuosity changes not only with the porosity, but as well with the distribution of the solid material presents in the investigated region. Another parameter that incide in the tortuosity is the shape and size of the obstacles.

### Acknowledgments

The current study is financially supported by the National Secretary of Higher Education Science, Technology and Innovation from Ecuador (Senescyt) which is gratefully acknowledged.

### References

1. S. Chen and G. Doolen, *Annu. Rev. Fluid Mech.*, **30**:329-64 (1998).
2. M. Sukop and D. Thorne, in *Lattice Boltzmann Modeling – And Introduction for Geoscientists and Engineers*, Springer-Verlag Berlin Heidelberg (2006).
3. A. Mohamed, in *Lattice Boltzmann Method Fundamentals and Engineering Applications with Computer Codes*, Springer-Verlag London, UK (2011).
4. H. Paradis, in *Micro- and Macroscale Modeling of Transport Processes in Solid Oxide Fuel Cells*, Lund University, Lund, Sweden, Ph.D. Thesis (2013).
5. P. Dhiraj, P. Kannan and B. Sanjoy, *Journal of Computational Physics*, **265**, 172 (2014).
6. Y. Yan, Y. Zu and B. Dong, *Applied Thermal Engineering*, **31** (2011).
7. T. Seta, E. Takegoshi and K. Okui, *Mathematics and Computers in Simulation*, **72**, 195 (2006).
8. M. Spaid and F. Phelan, *Phys. Fluids*, **9** (9), 2468 (1997).
9. D. Nield and A. Bejan, in *Convection in Porous Media*, Springer Science+Business Media, New York (2006).
10. A. Ghassemi and A. Pak, *Int. J. Numer. Anal. Meth. Geomech.*, (2010).
11. A. Nabovati and M. Sousa, *Journal of Engineering Science and Technology*, Vol. 2, No. 3, 226 (2007).
12. A. Koponen, M. Kataja and J. Timonen, *Physical Review E*, **54**(1), 406 (1996).
13. A. Koponen, M. Kataja and J. Timonen, *Physical Review E*, **56**(3), (1997).
14. M. Barrande, R. Bouchet and R. Denoyel, *Anal. Chem.*, **79**, 9115 (2007).
15. C. Spiegel, in *PEM Fuel Cell Modeling and Simulation Using Matlab*, Elsevier Inc. Oxford, UK (2008).
16. N. Brandon and D. Brett, *Phil. Trans. R. Soc.*, **364A**, 147 (2006).
17. M. Lee, J. Jung, K. Zhao, B. Kim, Q. Xu, B. Ahn and S. Kim, *Journal of the European Ceramic Society*, **34**, 1771 (2014).
18. D. Ingham and I. Pop, in *Transport Phenomena in porous Media III*, Elsevier Ltd., Oxford, UK (2005).
19. R. Roshandel, B. Farhanieh and E. Saievar-Iranizad, *Renewable Energy*, **30**(10), 1557 (2005).



20. A. Jena and K. Gupta, in *Characterization of Porosity of Electrodes and Separators in Fuel Cell Industry*, Porous Materials Inc. Report.
21. M. Ehrhardt, J. Fuhrmann, F. Holzbecher and A. Linke, *Weiertrass Institute for Applied Analysis and Stochastics. Berlin, Germany*, (2008).
22. Z. Zhang and L. Jia, *Int. J. Energy Res.*, **33**, 52 (2009).
23. J. Zhenjun and N. Shikazono, *Journal of The Electrochemical Society*, **160**(6), F709 (2013).
24. Y. Wang, J. Yuan, and B. Sundén, *Journal of Power Sources*, **254**, 209 (2014).
25. Y. Park and H. Kim, *Ceramics International*, **40**, 1447 (2014).
26. V. Schmidt and C. Tsai, *Journal of Power Sources*, **180**, 253 (2008).
27. A. Nabovati, J. Hinebaugh, A. Bazylak and C. Amon, *Journal of Power Sources*, **248**, 83 (2014).